JOURNAL OF SOLID STATE CHEMISTRY 49, 180–187 (1983)

Optical and ESR Investigations of Lanthanum Aluminates $LaMg_{1-x}Mn_xO_{19}$ Single Crystals with Magnetoplumbite-like Structure

F. LAVILLE, D. GOURIER, A. M. LEJUS,[1] AND D. VIVIEN

Laboratoire de Chimie Appliquée de l'Etat Solide, LA 302 CNRS, ENSCP 11 rue Pierre et Marie Curie, 75231 Paris Cedex 05, France

Received March 4, 1983

New lanthanum aluminates $LaMAl_{11}O_{19}$ (M^{2+} = Ni, Co, Mn, $Mg_{1-x}Mn_x$, $0 \leq x \leq 1$), with magnetoplumbite-like structure have been obtained as single crystals. This paper is particularly devoted to the Mn^{2+} and Mg^{2+}/Mn^{2+} mixed compounds, which exhibit promising luminescent properties. Several characteristics of the crystals are given. The absorption spectra of the materials, as grown, are assigned to Mn^{2+} ions in tetrahedral sites. After annealing in air new absorptions attributed to octahedral Mn^{3+} ions, appear. The ESR spectra of Mn^{2+} in all these crystals exhibit axial symmetry. For $x \leq 0.25$ they arise from isolated Mn^{2+} ions in slightly distorted tetrahedral sites and reveal a strong disorder effect. For $x \geq 0.5$ the spectra consist of a single line, attributed to clusters of magnetically interacting Mn^{2+} ions.

Introduction

Lanthanum aluminate with the approximate formula $LaAl_{11}O_{18}$ and magnesium stabilized aluminates $LnMgAl_{11}O_{19}$ with magnetoplumbite like structures have been proposed for a number of applications including their use as hosts for highly efficient phosphors (*1–5*) and for radioactive waste disposal (*6*). In the single crystal form, they may also be good substrates for LPE growth of rare earth hexaferrite thin films (*7*). Large single crystals of the compounds $LnMgAl_{11}O_{19}$ with Ln = La, Pr, Nd, Sm, Eu have recently been grown in this laboratory (*8, 9*). A refinement of the crystal structure of $LaMgAl_{11}O_{19}$ confirmed the magnetoplumbite character of these compounds. Their hexagonal unit cell consists of spinel blocks with Al(Mg) ions in tetrahedral and octahedral sites separated by mirror planes containing oxygen ions; the lanthanide and Al(Mg) cations are trigonal bipyramidly coordinated. However, it was impossible in the X-ray study to distinguish between Al and Mg because they have identical X-ray scattering factors. It should be pointed out that the solid state synthesis of $LaMgAl_{11}O_{19}$ is much easier than the $LaAl_{11}O_{18}$ one, and that the presence of MgO in the starting mixture of oxides appears essential to obtain large single crystals of aluminates. Clearly, Mg^{2+} cations play an important role in this magnetoplumbite structure. Other divalent ions M, such as Mn, Fe, Co, Ni, can also enter the magnetoplumbite phase $LaMAl_{11}O_{19}$ (*8*). Obtaining single crystals of these com-

[1] To whom all correspondence should be addressed.

0022-4596/83 $3.00

pounds would allow determination at the localization of the transition metal cations either by X-ray diffraction (unlike Mg^{2+}, they can be distinguished from Al^{3+}), or by several spectroscopic technics. The role and properties of these ions in the magnetoplumbite structure will then become more clear.

This paper reports on the preparation and characterization of large single crystals of these transition metal ion "stabilized" phases. It deals particularly with the Mn^{2+} and Mg/Mn mixed compounds which look very promising as green emitting phosphors (4). Prior to this time these materials have only been synthesized in the powder form by solid state reactions. The uv–visible absorption and EPR spectra of these compounds will also be discussed. Their crystal structures and luminescence properties are currently under investigation.

Crystal Growth and Characterization

Single crystals of lanthanum aluminates have been grown from the melt ($T_f \cong$ 1800°C), using either the Verneuil process (flame fusion method) or the floating zone method. Our Verneuil apparatus and crystal growth procedure have been described elsewhere (*10*). The starting material is an intimate mixture of the oxides γ-Al_2O_3, La_2O_3, and MO_x with M = Ni, Mn, Co, Mg/Mn. The reducing power of the oxyhydrogen torch can be adjusted to convert or maintain "M" in the divalent state. For example, to prepare $LaMnAl_{11}O_{19}$, the starting oxide MnO_2 must be reduced into MnO, when passing through the flame. Therefore the torch operates with a more reducing flame (H_2 flow = 13 liters/min, O_2 flow = 4 liters/min) than for growing $LaMgAl_{11}O_{19}$ crystals (H_2 = 11.7 liters/min, O_2 = 4.5 liters/min). Samples prepared by this process are rod-shaped 5–10 mm diameter, 20–50 mm long. They are constituted of several large crystals, typically 10 × 5 × 2 mm^3 in size. The floating zone method, in air, is carried out in a light-focusing furnace (*11*). The rod-shaped crystals are 5 mm in diameter, 20–30 mm long (Fig. 1a).

These two methods have allowed us to

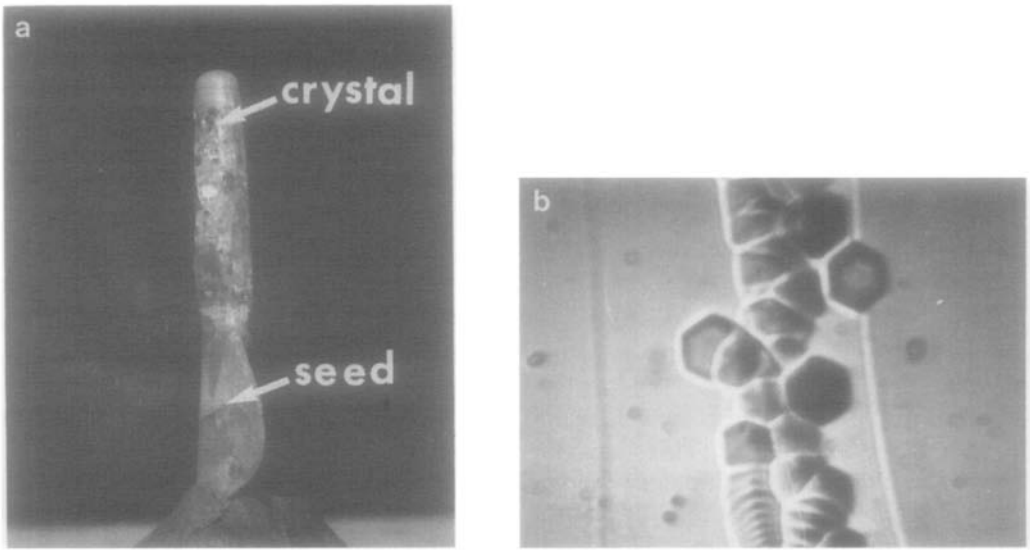

FIG. 1. (a) Crystal of $LaMg_{0.98}Mn_{0.02}Al_{11}O_{19}$ prepared by the floating zone method (G = 1.5). (b) Hexagonal etch pits on a cleavage plane (0001) of this crystal (G = 600).

synthesize large single crystals of $LaMg_{1-x}Mn_xAl_{11}O_{19}$ for the following values of x: 0, 0.005, 0.02, 0.05, 0.10, 0.25, 0.50, 0.75, 0.85, 0.90, 0.95, 1. These crystals, which were initially green turn pink upon annealing in air at 1400°C for 1 week.

Other single crystals, such as $LaNiAl_{11}O_{19}$ and $LaCoAl_{11}O_{19}$, have also been obtained by using the Verneuil process. Their crystal growth and characterization will be described elsewhere (*12*).

The Debye–Scherrer powder diagrams of the compounds are similar to those of $LaMgAl_{11}O_{19}$ with a magnetoplumbite-type structure (9). The unit-cell parameters a = 5.59 Å and c = 21.99 Å are independent of x, except for the c parameter which slightly increases up to 22.036 Å when $x \geq 0.85$.

Crystals thus grown exhibit imperfections such as cracks and microbubbles. However, despite their mosaic structure, they contain large areas with good crystalline quality (Laüe tests). For both methods the growth axis is the **a** direction which lies in the cleavage plane of the crystals.

The crystals show a good chemical stability and are completely inert toward most of acids and alkaline solutions. Dipping the crystals, for at least 20 min, in boiling H_3PO_4 leads to the formation of hexagonal etch pits on the cleavage plane (Fig. 1b).

Microhardness measurements have been performed by the Knoop process. This is the most suitable method because of the brittle character of the crystals. The results are presented Table I. Microhardness is isotropic in the basal planes and strongly anisotropic in prismatic ones. The hardness measured along [0001] is greater than the one along $\langle 10\bar{1}0 \rangle$. However, the highest value is observed for a direction whose angle with the **c** axis is 35°. This behavior seems to be characteristic of magnetoplumbite type aluminates. On the contrary for the related β-alumina family, microhardness is maximum along the **c** axis (*13*).

The uv–vis absorption spectra of $LaMg_{1-x}Mn_xAl_{11}O_{19}$ (x = 0.02, 0.05, 0.1, 0.25, 0.50, 0.75, 1) have been recorded on the as grown and air-annealed single crystals using PYE-UNICAM SP 1800 or BECKMAN UV 5270 spectrometers. Small single crystalline platelets about 1 mm thick were mounted with their **c** crystal axis coincident with the light beam direction.

TABLE I

MICROHARDNESS H (kg/mm²) OF $LaMg_{1-x}Mn_xAl_{11}O_{19}$ SINGLE CRYSTALS IN BASAL (0001) AND PRISMATIC $\{10\bar{1}0\}$ PLANES (100-g LOAD APPLIED FOR 10 sec)

x	r^a (Å)	(0001)	$\{10\bar{1}0\}$		
			$H_{\parallel[0001]}$	H_{Max}	$H_{\parallel\langle 10\bar{1}0\rangle}$
0	0.66	1400	1660	1900	1300
1	0.80	1385	1500	1840	1450

[a] Ionic radius of Mg or Mn ions.

The ESR spectra of $LaMg_{1-x}Mn_xAl_{11}O_{19}$ single crystals have been recorded on JEOL ME 3X or BRUCKER 220 D spectrometers operating at X band and room temperature. The magnetic field was calibrated using a Brucker BNM 12 NMR proton probe, and the klystron frequency measured with a SYSTRON DONNER microwave frequency counter.

Absorption Spectra of the Manganese Compounds

For $x \geq 0.1$, all the spectra of the as grown green colored crystals look identical. There is no significant improvement of their resolution by lowering the temperature of the samples down to 110 K. The spectrum corresponding to x = 1 is given in Fig. 2a. All the observed lines can be fitted to the Tanabe-Sugano interaction matrix (*14*) of a d^5 ion (thus confirming that manganese is in the 2+ oxidation state) in octahedral or tetrahedral symmetry. The experimental and calculated wavelengths of the spectral lines, together with their assignment are

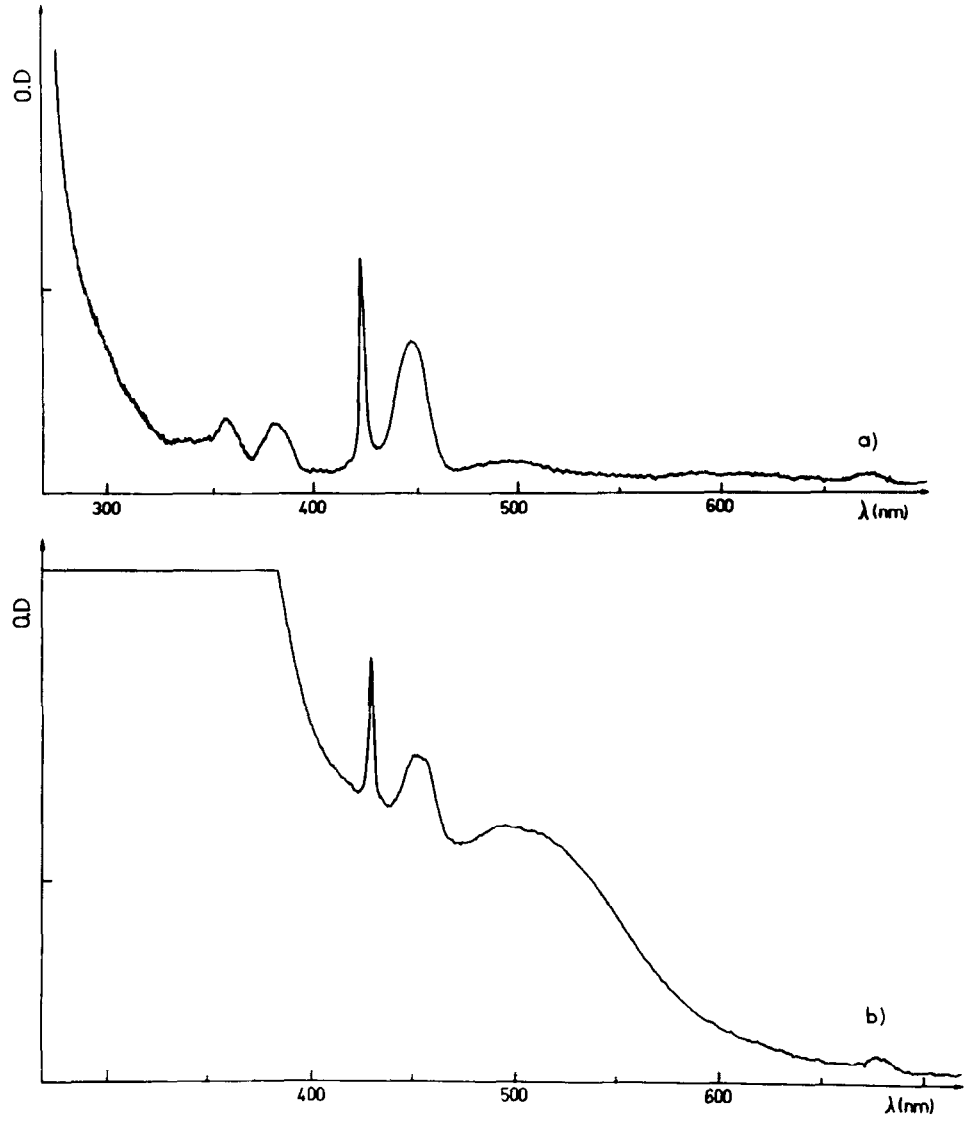

FIG. 2. (a) Absorption spectrum of an as grown green $LaMnAl_{11}O_{19}$ crystal. The light propagates along the c axis. (b) Same crystal after air annealing at 1400°C for 1 week.

given in Table II. Using $B = 571\ cm^{-1}$, $B/C = 0.160$, and $Dq = 566\ cm^{-1}$, the RMS deviation of the fitting is 2.7 nm. These parameters are quite similar to those found by Tamatani (*1*) for manganese in the magnetoplumbite aluminate host "La_2O_3, 11 Al_2O_3," but rather different from those reported for Mn^{2+}: sodium β-alumina by Akridge and Kennedy (*15*). This could indicate that the Mn^{2+} ions are sensitive to the composition of the mirror plane which distinguishes between β-alumina and magnetoplumbite structures. However, the Dq value indicates that Mn^{2+} ions are localized in tetrahedral positions (*15, 16*). Octahedral crystal fields will give 10 Dq values in

TABLE II

EXPERIMENTAL AND CALCULATED TRANSITIONS OF THE ABSORPTION SPECTRUM OF Mn^{2+} IN $LaMg_{1-x}Mn_xAl_{11}O_{19}$ ($x \geq 0.1$)[a]

	Excited state				
	^4E (^4D)	$^4T_2$ (^4D)	$^4A_1$ (^4D) ^4E	$^4T_2$ (^4G)	$^4T_1$ (^4G)
λ_{exp} (nm)	358.5	381.5	425.5	449.5	492.5
λ_{calc} (nm)	362.9	378.7	424.5	446.9	493.8

[a] The ground state is the $^6A_1$ level.

the range 8500–9000 cm^{-1}. It should be noticed that there are no evidence of octahedral manganese in the absorption spectra, whatever the value of x, though Stevels (*5*) has suggested its existence in "$La_{1-y}Eu_yMgMn_xAl_{11+y/3-2x/3}O_{19}$" for $x > 0.15$ prepared in powdered form by solid state reactions. However, the octahedral manganese lines should be much weaker than the tetrahedral ones and therefore must be unobservable. Magnetic circular dichroism investigation of these crystals may reveal such weak lines. It should be pointed out that the 492.5-nm band of the spectrum is rather broad. A lowering of the tetrahedral symmetry to C_{3v} or C_s for example, which splits the $^4T_1$ level could explain this observation. However, further investigation of the exact symmetry of the manganese sites will require polarized spectra which are not available at present.

The tetrahedral localization of Mn^{2+} is confirmed by the intense green light emitted by all the samples with $x \geq 0.02$ under either uv or X-ray excitation. This transition which arises between the $^4T_1$ (^4G) and $^6A_1$ (^6S) levels generally lies in the green region of the visible spectrum for tetrahedral manganese (*16*), (4) and in the orange to red for the octahedral one (*17*), (5).

In the spectra of the pink air annealed crystals (Fig. 2b) the lines of tetrahedral manganese are still present, although less intense, and new absorptions appear in the 500-nm region, with maxima at 490 and 515 nm and there is a red shift of about 100 nm of the uv absorption edge of the crystal. The bands near 500 nm are attributed to the transition $^5E \rightarrow {}^5T_2$ of octahedral Mn^{3+} ions (*18; 19,* and reference therein) split because of a small deviation from the true O_h symmetry. The Mn^{3+} transitions should be far more intense than the Mn^{2+} ones because they are spin allowed. Hence, just a small part of the Mn^{2+} ions needs to be oxidized to explain the new absorption lines. One cannot say if these Mn^{3+} ions come from manganeous ions which were initially located in octahedral environment, or if migration from tetrahedral to octahedral sites has occured simultaneously with the manganese oxidation during the crystals annealing.

Concerning the red shift of the absorption edge of the pink crystals, it should be pointed out that annealing pure $LaMgAl_{11}O_{19}$ does not produce such a shift. It follows that it has to be associated with Mn^{3+} ions. Oxygen to Mn^{3+} charge transfer bands can be very intense. It is known that when the charge of a metal ion in a complex increases, the ligand to metal charge transfer bands are red shifted (*7*). This probably explains the difference in the absorption edge of the green and pink crystals.

ESR Study

As grown and air annealed crystals give essentially the same ESR spectra (although slightly less intense for the latter ones). These spectra originate from the $S = \frac{5}{2}$, $I = \frac{5}{2}$ Mn^{2+} ions while the non Kramer Mn^{3+} ions of the air annealed samples are undetectable with our experimental setting. The spectra of all the crystals exhibit axial symmetry around the **c** crystal direction, but their shapes depend on the manganese content of the samples (Fig. 3).

For $x \leq 0.25$ the spectra which consist mainly of six hyperfine lines corresponding

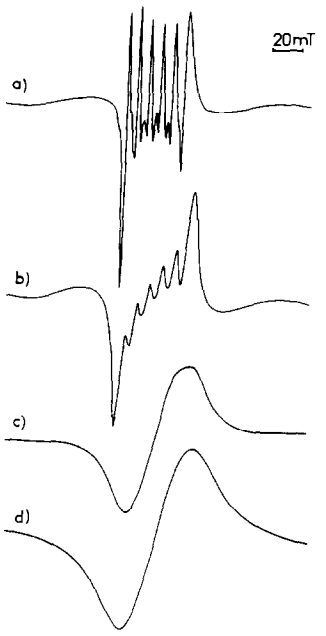

FIG. 3. Evolution of the parallel ESR spectrum of $LaMg_{1-x}Mn_xAl_{11}O_{19}$ crystals. (a) $x = 0.10$, (b) $x = 0.25$, (c) $x = 0.50$, (d) $x = 1$.

to the $M_S = \frac{1}{2} \leftrightarrow -\frac{1}{2}$ transition, arise from isolated Mn^{2+} ions. For $x \geq 0.5$ one observes only a single and approximately lorentzian line characteristic of manganese clusters with magnetic exchange interaction between Mn^{2+} ions.

Spectra of Isolated Mn^{2+} Ions

Figures 3a and b shows that the linewidth of the isolated Mn^{2+} ESR lines increases with x. This arises because of the dipolar interaction between paramagnetic ions, whose magnitude increases when the Mn^{2+}–Mn^{2+} distances decrease. However, the intensity of the ESR lines is always maximum where B_0 is along the **c** crystal axis, and the spectra are isotropic when B_0 rotates in a plane perpendicular to **c**. Thus, the Mn^{2+} sites exhibit axial symmetry with $z \parallel \mathbf{c}$. If we assume that Mn^{2+} ions occupy normal cationic sites of the magnetoplumbite structure, the axial character of the spectrum with $z \parallel \mathbf{c}$ supports a localization of Mn^{2+} in the $4f$ (in Wyckoff notation) tetrahedral sites in the spinel blocks with C_{3v} point group symmetry. Such a localization is in good agreement with the optical study. Occupancy of the 12 k octahedral sites of the spinel blocks, with C_{2v} real symmetry, would have introduced some orthorhombic character to the ESR spectrum, but interstitial sites, or the normal "$2b$" cationic site of the magnetoplumbite mirror plane with trigonal bipyramid coordination could also account for axial symmetry.

The striking feature of these spectra is the absence of resolved $M_S = \pm\frac{3}{2} \leftrightarrow \pm\frac{5}{2}$ and $\pm\frac{1}{2} \leftrightarrow \pm\frac{3}{2}$ fine structure lines, these latter appearing only as two bumps (Fig. 4b) flanking the central $M_S = -\frac{1}{2} \leftrightarrow +\frac{1}{2}$ transition in the perpendicular spectrum. Furthermore, in the parallel spectrum, B_0 being parallel to a principal direction of the D tensor along which they should vanish (*21*), strong forbidden lines appear between the six allowed ones in the $M_S = \frac{1}{2} \leftrightarrow -\frac{1}{2}$ transition (Fig. 4a). A similar behavior has already been noticed in sodium β-alumina

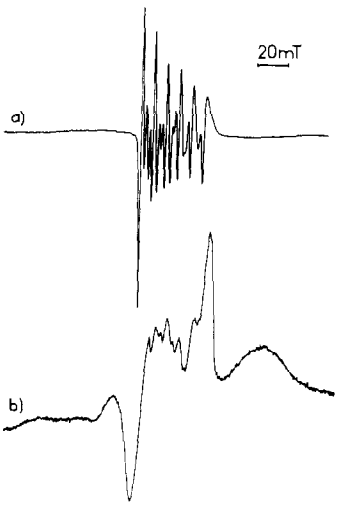

FIG. 4. X Band ESR spectra of Mn^{2+} in $LaMg_{0.98}Mn_{0.02}Al_{11}O_{19}$. (a) $B_0 \parallel c$, (b) $B_0 \perp c$. Note the strong forbidden hyperfine lines in (a) and the broadness of the outer fine structure lines in (b).

doped with Mn^{2+} (*22, 23*), the doping ion being introduced at the crystal synthesis stage, and not by ion exchange of Na^+ ions (*24*). This arises because of spreads ΔD and $\Delta\Theta$ of the axial zero field parameter D, and of the angle Θ between the z zero field tensor axis and the **c** crystal direction. An estimation of the mean D value of the manganese ions can be extracted from the spacings of the forbidden lines of the parallel spectrum (Table III) by the usual procedure (*23, 25*).

Taking $A_{\parallel} = A_{\perp} = 0.2$ mT and $g = 2.01$, a least squares fitting of D and P (the axial electric quadrupole interaction parameter) over the four experimental spacings leads to the values:

$$D = -49.55 \text{ mT} \quad (465 \times 10^{-4} \text{ cm}^{-1})$$
$$P = 0.0036 \text{ mT}.$$

The D value is very different from those found for Mn^{2+} in Na β-alumina: -19.4 mT (*22*) or -38.6 mT (*23*).

This indicates that the manganese sites in the magnetoplumbite structure are more distorted from the regular tetrahedral symmetry than in the β-alumina one. Using the D value, one can determine the distribution ΔD of D which contributes to the anisotropy of the linewidth and to the broadening of the outer fine structure lines using the expression derived by Barklie (*2*),

$$\Delta D = \frac{B_0}{4|D|} (\Delta B_{90} - \Delta B_0)$$

where B_0 is the central field, ΔB_0 and ΔB_{90} the mean linewidths of the $M_S = \frac{1}{2} \leftrightarrow -\frac{1}{2}$ at $\Theta = 0$ and $\Theta = 90°$, respectively. ΔB_0 must be deduced from a computer simulation of the spectrum because of the broadness of the lines.

Taking $\Delta B_0 = 1.6$ mT and $\Delta B_{90} = 7.5$ mT for $x = 0.02$ it follows $\Delta D = 9.8$ mT.

The reasons which lead to such a spread in D value are not fully understood at present. However, one can infer that it arises from the presence of cationic and anionic vacancies in the structure, in the vicinity of the Mn^{2+} ions. Indeed, we have recently shown (*26*) that the magnetoplumbite structure with theoretical formula $LaMgAl_{11}O_{19}$ can accommodate a rather large deficiency in lanthanum, magnesium, or aluminum, with simultaneous formation of oxygen vacancies.

Such a defective structure is likely to occur spontaneously even in the "stoichiometric" material because some volatile reduced species such as metallic Mg for instance can be formed in the oxyhdric torch during the crystal growth procedure. However, we cannot rule out a contribution of a statistical distribution of manganese among several sites to ΔD and $\Delta\Theta$.

TABLE III

EXPERIMENTAL AND CALCULATED SPACING ΔB_f (mT) OF THE FORBIDDEN HYPERFINE TRANSITIONS $|M_s, m_I - 1> \leftrightarrow |M_s - 1, m_I>$ AND $|M_s, m_I> \leftrightarrow |M_s - 1, m_I - 1>$ ACCORDING TO THE m_I VALUE, FOR THE $M_s = \frac{1}{2} \leftrightarrow -\frac{1}{2}$ TRANSITION OF THE PARALLEL SPECTRUM OF $LaMg_{0.98}Mn_{0.02}Al_{11}O_{19}$

	m_I				
	$-\frac{3}{2}$	$-\frac{1}{2}$	$\frac{1}{2}$	$\frac{3}{2}$	$\frac{5}{2}$
$\Delta B_{f,exp}$	2.73	2.28	1.93	1.69	[a]
$\Delta B_{f,calc}$	2.70	2.36	2.01	1.67	1.33

[a] Line overlapping preclude precise measurement of this spacing.

Spectra of the Mn^{2+} Clusters

For all the orientations of the magnetic field with respect to the crystal axis, the ESR spectra of the $x \geq 0.5$ crystals (Figs. 3c and d) consist of a single line. This line, slightly asymmetric for $x = 0.5$ and 0.75, becomes approximately Lorentzian for $x = 1$ (Fig. 3d). The spectra are of axial symmetry with a small anisotropy in the g factor and linewidth ΔB. The principal values of

these parameters for $LaMnAl_{11}O_{19}$ are

$$g_{\parallel} = 2.027$$

$$g_{\perp} = 2.017$$

$$\Delta B_{\parallel} = 38.8 \text{ mT}$$

$$\Delta B_{\perp} = 36.3 \text{ mT}.$$

These ESR spectra must be attributed to clusters of magnetically interacting Mn^{2+} ions (*21, 27, 28*). The lines are relatively narrow and approximately Lorentzian. This indicates that the exchange interaction is larger than the dipolar interaction (*28*). The g values too, which are slightly higher than those of isolated Mn^{2+} ions, probably reflect local magnetic fields due to magnetically interacting ions (*29*). It should be noticed that when the manganese content in $LaMg_{1-x}Mn_xAl_{11}O_{19}$ increases, one goes directly from isolated Mn^{2+} ions to clusters. There is no intermediate formation, for instance, of manganese pairs (*27*). This is in favor of a statistical distribution of the Mn^{2+} ions among all its possible sites in the compound.

References

1. M. Tamatani, *Jpn. J. Appl. Phys.* **13,** 950 (1974).
2. J. M. P. J. Verstegen, J. L. Sommerdijk, and J. G. Verriet, *J. Lumin.* **6,** 425 (1973).
3. A. L. N. Stevels and A. D. M. Schrama de Pauw, *J. Electrochem. Soc.* **123,** 691 (1976).
4. A. L. N. Stevels and J. M. P. J. Verstegen, *J. Lumin.* **14,** 207 (1976).
5. A. L. N. Stevels, *J. Lumin.* **20,** 99 (1979).
6. P. E. D. Morgan, D. R. Clarke, C. M. Jantzen, and A. B. Harker, *J. Am. Ceram. Soc.* **64,** 249 (1981); C. M. Jantzen, R. R. Neurgaonkar, *Mater. Res. Bull.* **16,** 519 (1981).
7. F. Haberey, R. Leckebusch, M. Rosenberg, and K. Sahl, *Naturwissenschaften* **68,** 376 (1981).
8. A. Kahn, A. M. Lejus, M. Madsac, J. Thery, and D. Vivien, *J. Appl. Phys.* **52,** 6864 (1981).
9. D. Saber and A. M. Lejus, *Mater. Res. Bull.* **16,** 1325 (1981).
10. A. M. Lejus and J. P. Connan, *Rev. Int. Hautes Temp. Réfract.* **11,** 215 (1974).
11. A. Revcolevschi, *Rev. Int. Hautes Temp. Réfract.* **7,** 73 (1970).
12. F. Laville and A. M. Lejus, to be published.
13. J. Thery and A. M. Lejus, *Mater. Res. Bull.*, to be published.
14. J. S. Griffith, "The Theory of Transition Metal Ions," p. 44, Cambridge Univ. Press, London/New York (1961).
15. J. R. Akridge and J. H. Kennedy, *J. Solid State Chem.* **29,** 63 (1979).
16. D. T. Palumbo and J. J. Brown Jr., *J. Electrochem. Soc.* **117,** 1184 (1970).
17. D. T. Palumbo and J. J. Brown Jr., *J. Electrochem. Soc.* **118,** 1159 (1971).
18. A. T. Kai, S. Larsson, and U. Halenius, *Phys. Chem. Miner.* **6,** 77 (1980).
19. G. Smith, U. Halenius, and K. Langer, *Phys. Chem. Miner.* **8,** 136 (1982).
20. A. B. P. Lever, *J. Chem. Educ.* **51,** 612 (1974).
21. A. Abragam and B. Bleaney, "Résonance Paramagnétique Électronique des Ions de Transition" (French translation) PUF, Paris (1971).
22. R. C. Barklie and K. O'Donnel, *J. Phys. C* **10,** 4127 (1977).
23. Ph. Colomban and D. Vivien, *Phys. Status Solidi A* **76**(2) 565 (1983).
24. J. Antoine, D. Vivien, J. Livage, J. Thery, and R. Collongues, *Mater. Res. Bull.* **10,** 865 (1975).
25. H. W. de Wijn and R. F. van Balderen, *J. Chem. Phys.* **46,** 1381 (1967).
26. C. Damerval, Diplôme d'Etudes Superieures, Université de Paris (1982), to be published.
27. J. Owen and E. A. Harris, *in* "Electron Paramagnetic Resonance," (S. Geschwind, Ed.), p. 427, Plenum, New York (1972).
28. G. A. Korteweg and L. L. van Reijen, *J. Magn. Res.* **44,** 159 (1981).
29. D. Vivien, A. M. Lejus, and R. Collongues, *Nouv. J. Chim.* **2,** 569 (1978).